LA-UR -77-2530

CONF-771061--2

TITLE: DAMAGE RESISTANCE OF AR-COATED GERMANIUM SURFACES FOR NANOSECOND CO_2 LASER PULSES

AUTHOR(S): Brian E. Newnam, AP-2

Dennis H. Gill, AP-2

MASTER

SUBMITTED TO: Proceedings of: 1977 Symposium on Optical Materials for High Power Lasers (Damage Symposium).

los alamos scientific laboratory
of the University of California
LOS ALAMOS, NEW MEXICO 87545

An Affirmative Action/Equal Opportunity Employer

Form No. 836
St. No. 2629
1/75

UNITED STATES
ENERGY RESEARCH AND
DEVELOPMENT ADMINISTRATION
CONTRACT W-7405-ENG. 36

DISTRIBUTION ... UNLIMITED

DAMAGE RESISTANCE OF AR-COATED GERMANIUM SURFACES FOR NANOSECOND CO_2 LASER PULSES*

Brian E. Newnam and Dennis H. Gill
Los Alamos Scientific Laboratory
Los Alamos, New Mexico 87545

An evaluation of the state-of-the-art of AR coatings on gallium-doped germanium, used as a saturable absorber at 10.6 µm, has been conducted. Both 1-on-1 and N-on-1 laser damage thresholds were measured with 1.2 ns pulses on bare and coated surfaces. Only front surface damage was observed. With few exceptions, the thresholds for coated surfaces were centered at 0.49 ± 0.3 J/cm^2. Bare Ge had a threshold ranging from 0.65 to 0.70 J/cm^2. No significant differences due to substrate polish, crystallinity or doping level were evident and multiple-shot conditioning resulted in the same threshold as for single shot tests. From an analysis of standing-wave electric fields, damage or AR-coated GE appeared to be limited by the surface properties of Ge. Measurements at both 1.2 and 70 ns indicated that the threshold (J/cm^2) of both coated and uncoated Ge increases as the square root of the pulsewidth.

Key words: Antireflection coatings, germanium, laser damage, saturable absorber, standing-wave electric field.

1. Introduction

Gallium-doped germanium has been developed for use as a saturable absorber to prevent pre-pulse gain depletion in the large CO_2 amplifiers of LASL's eight-beam fusion laser [1,2]. For use at saturating intensities for pulses 1-nanosecond in duration, the damage resistance of the AR-coated surfaces must be maximized. Accordingly, a careful evaluation of the state-of-the-art of AR coatings at 10.6 µm was performed.

Antireflection coatings comprising fourteen coating designs using eight film materials were obtained from nine coating manufacturers. Polycrystalline, p-doped Ge substrates polished by one vendor were supplied to each. Substrates polished by a second vendor were also supplied for comparision. Additionally, single-crystal Ge, p-doped and undoped, and undoped polycrystalline Ge were coated by one vendor to evaluate the effect of crystal structure and doping. The dimensions of the test substrates were 25 mm in diameter and 6 mm thick. Coating depositions, however, were performed in chambers large enough to eventually coat amplifier-size Ge discs (41-cm diameter and 4-cm thickness) with sufficient uniformity to obtain a reflectance per surface of less than 1% at 10.6 µm and less than 3% from 9 to 11 µm.

2. Experimental Procedure

Laser damage tests were conducted with 1.15 ± 0.05 ns pulses (FWHM) at the P(20) 10.6 µm wavelength. These short pulses were reliably carved out of a smoothed gain-switched pulse by use of a Pockel cell arrangement. The scematic of the laser diagnostics is shown in figure 1. Pulsewidth measurements were made with a Molectron pyroelectric detector coupled to a 5 GHz bandwidth oscilloscope of LASL design [3]. For supplementary tests with a 70-ns pulsewidth, a photon-drag detector was used. Oscillograms of the temporal pulses are shown in figure 2.

The test samples were located prior to the focus of a 1 m F.L. ZnSe lens where the beam spot-size radius was 1.0 mm. The peak value of the irradiance (J/cm^2) at the sample plane was measured on each shot by use of a 197-µm diameter pinhole (Optimation, Inc.). The pinhole was located in a split-off beam and placed at the same distance from an identical ZnSe lens as was the sample. The energy transmitted by the pinhole at the center of the reference laser beam was measured by a Laser Precision Energy Meter (isolated from rf noise). Prior to each test series a calibration was performed with an identical 197-µm pinhole centered at the sample plane. During the damage tests the reproducibility of the spatial profile was monitored by comparing the energy focussed through the pinhole reference with the total energy measured by a Scientech calorimeter. The 197-µm diameter of the pinhole was chosen to minimize the spatial averaging over the beam profile (at the pinhole perimeter the intensity of the Gaussian profile dropped to 98% of the peak value) while transmitting an adequate amount of energy for easy detection. Also, the ratio of the pinhole diameter to the wavelength was large enough to avoid significant diffraction effects. By use of the equation,

$$T = 1 - \frac{1}{\pi(ka)^{3/2}} \sin(2ka - \frac{\pi}{4}) + \qquad (1)$$

*Work supported by the U. S. Department of Energy.

1 Figures in brackets indicate the literature references at the end of this paper.

where a = aperture radius [4], the transmittance of the 197 μm-diameter aperture was calculated to be 99.98%.

Damage was detected visually by the onset of increased surface scattering of a He-Ne laser beam directed on the same site (back and front) as the pulsed laser and by examination under bright white-light illumination using the He-Ne beam as the locator. After the tests, examination of irradiated areas was also performed with a microscope (300X).

3. Damage Morphology

The characteristics of the laser-damaged sites viewed under 200 and 300 X magnification were very interesting. Only front surface damage was observed in these tests. In figure 3, disruption of an AR-coated ($Ge/PbF_2/ZnSe/Au$) surface of p-doped, polycrystalline Ge caused by a single 1-ns pulse above threshold is examined. The AR-coating has been removed rather uniformly leaving a well-defined perimeter. Linear interference ripples oriented normal to the laser polarization are grouped around circular damage pits. Temple and Soileau have identified these ripples as perturbations in the surface toptography due to interference of the incident laser electric field with the time-varying (laser frequency) induced surface charges on surface scratches, voids and inclusions [5]. The diameter of the pits are mostly 8 to 12 μm and the ripple spacing is approximately 5.5 μm which are close to the laser wavelength. Damage sites in uncoated Ge (not shown) caused by 1-ns pulses did have faint ripples of exactly (± .2 μm) the laser wavelength (10.6 μm) spacing.

The morphology of damage caused by 70-ns pulses was very different from the above as shown in figure 4. On the coated surface, a random distribution of irregular sites was related to damage at defect sites, and extensive cracking of the AR coating is probably thermally-caused by delamination. For bare Ge (fig. 5) the damage sites were all centered on circular pits and very tightly-spaced (1.6 μm) interference fringes parallel to the laser polarization. The cause of these fringes has not been identified.

4. Results

The experimental results for coated and bare Ge substrates are presented in table 1-3. These thresholds are for pit formation or film disruption which occurred at much lower intensities than a breakdown plasma. Only the mean value of each thresholdis listed for the coated surfaces since the range, typically ± 0.02 or less, was unusually small. The absolute accuracy is considered to be ± 10%. All thresholds listed are for front surface damage only as we were unable to damage any rear surface, coated or uncoated. Further, we observed no difference between thresholds for 1-on-1 and N-on-1 tests, where N-1 shots (10 to 15) were fired below the single-shot threshold before, irradiating with a damaging intensity.

To compare the effects of two different conventional polishing methods, single-and polycrystalline substrate material and Ga-doping level (undoped, R = 30 Ω·cm; doped, 5 Ω·cm), one coating vendor deposited a two-layer ThF_4/ZnS Vee-coat on each substrate during one run. As seen in table 1, no significant differences in thresholds caused by the two polishing methods were manifest. This was surprising since Polish A qualified as better than "40-20" (scratch and dig code), and Polish B was slightly worse than "40-20". Likewise, no real differences were measured between coated single-crystal and polycrystal Ge surfaces. Gallium-doping had no effect on coated single-crystal thresholds, and only a minor 10-15% threshold reduction was measured for Ga-doped polycrystalline Ge.

Table 1. Damage threshold of AR-coated Germanium substrates

Coating: $s/ThF_4/ZnS/a$

Germanium Substrate	Energy Density (J/cm^2) Polish A	Polish B
Single Crystal (undoped)	0.47	0.46
Single Crystal (P-doped)	0.47	0.46
Polycrystal (undoped)	0.48	0.51
Polycrystal (P-doped)	0.41	0.46

The thresholds for fourteen coating designs on P-doped, polycrystalline Ge are listed in table 2. Multiple entires represent different samples of the same coating. The values ranged from 0.41 to 0.5[illegible] J/cm^2 and the mean values was 0.49 ± 0.03 J/cm^2. Even the two-layer coating of $CaF_2/ZnSe$ had the same threshold despite the fact that CaF_2 has a large absorption coefficient at 10.6 μm.

Table 2. Damage thresholds of AR-coated Germanium

Vendor	Design	Energy Density (J/cm^2)
	one-layer coatings Ge/coating/Air	
I	ZnS	0.51, 0.46
E	ZnS	0.50, 0.47, 0.49[a]
D	TlI	0.46
	Two-layer coatings	
G	CaF_2/ZnSe	0.50, 0.48
H	PbF_2/ZnSe	0.49
E	ZnSe/ThF_4	0.48, 0.46
H	ThF_4/ZnSe	0.44
A	ThF_4/ZnS	0.46, 0.41
	Three-layer coatings Ge/Coating/Air	
I	ZnS/Ge/ZnS	0.53, 0.50
D	TlI/Kcl/TlI	0.50
F	ThF_4/ZnS/ThF_4	0.51, 0.48
F	ThF_4/ZnSe/ThF_4	0.50
E	ZnS/ThF_4/ZnS	0.48, 0.47
	Four- and Five-Layer Coatings	
C	ZnS/Ge/ZnS/ThF_4	0.57, 0.55, 0.51
B	ThF_4/ZnS/ThF_4/ZnS/ThF_4	0.47, 0.45

a Extra Ge substrate, undoped, polycrystalline, poor polish

Due to the relative unfiormity of thresholds for coated Ge surfaces, particular attention was paid to the thresholds of uncoated Ge presented in table 3. The values for three different bare surfaces were all greater than those of coated Ge by about 40%. In addition, it is noted that Ga-doping lowered the threshold by ~ 10%.

Table 3. Damage thresholds of uncoated polycrystalline Germanium (Front Surface Only)

	Energy Density (J/cm^2)
Undoped	0.70 ± 0.05
P-doped (Gallium)	0.65 ± 0.05
P-doped -HNO_3 treated	0.72 ± 0.05

The experimental results indicate that the damage threshold of AR coated Ge surfaces is 1) independent of the design and materials of the AR coatings and is 2) lower than uncoated Ge. Furthermore, damage occurred only at the front surface. These results may be explained by considering the electric fields in the Ge, coated and uncoated. Figure 6 represents the standing-wave electric fields, normalized to the incident field E_o^+, in the vicinity of the front surface of an AR-coated and uncoated

Ge substrate. Although, the exact field distribution within the AR coating must be calculated for each design, the gradual decrease of $|E/E_o^+|^2$ from 1.0 at the air-film interface to 0.25 at the film-Ge interface is the same for any design.

The normalized field in the AR coated substrate is easily calculated using the relation

$$\left|\frac{E_s}{E_o^+}\right|^2 = \frac{1}{n_s} \qquad (2)$$

where, for Ge, n_s = 4.0 at 10.6 µm.

Likewise, the field-squared in the uncoated Ge substrate, is 0.16 in the vicinity of the front surface as calculated from

$$\left|\frac{E_s}{E_o^+}\right|^2 = \frac{4}{(n_s H)^2} \qquad (3)$$

Since the power absorbed per cm^3 is given by

$$P_a = n\alpha |E/E_o^+|^2 \qquad (4)$$

for linear absorption, damage by this mechanism (or any other involving the electric field) in Ge would predictably occur at a lower incident laser intensity for an AR coated surface. The ratio of the fields squared in uncoated-to-coated Ge is computed to be 0.64. The ratio of the measured damage thresholds is 0.7 ± 0.1, which is consistent. These results indicate that the damage probably occurred in the Ge and the Ge/film interface. This, for all but the lowest thresholds measured, it is apparent that the coatings had at least as high damage resistance as the substrate itself.

It is informative to calculate the peak electric field present in the various coating materials at the threshold of damage of the coated Ge surfaces. These fields, listed in table 4, represent a number of samples and coating designs. In terms of electric field, it is seen that the same value, 0.2 MV/cm, existed in the coated and uncoated Ge substrates at the threshold, again implicating the substrate as the limiting factor.

Table 4. Peak electric field at damage threshold of coated Ge surfaces

Coating Material	Number of Samples	10.6 µm, 1.15 ns pulse E_{RMS} (MV/cm)
ZnS	17	0.33 to 0.40
ZnSe	7	0.33 to 0.40
TlI	2	0.32 to 0.39
ThF_4	15	0.24 to 0.40
PbF_2	1	0.33
CaF_2	2	0.30
KCl	1	0.23
Ge	2	0.22 to 0.26
Ge substrate coated	26	0.18 to 0.21
Ge substrate uncoated	7	0.18 to 0.19

It is interesting that the Ge films withstood 20 to 25% more electric field than the substrate. In most other cases, thin films are generally less damage-resistant than bulk material. Given a more damage resistant substrate than Ge, it is likely that the various coating components could survive even higher electric fields than attained in these tests.

6. Pulsewidth Dependence

A second set of tests at a longer pulsewidth, ~ 70 ns, produced thresholds of 4.2 J/cm^2 for PbF_2/ZnSe AR-coated Ge and 6.4 J/cm^2 for uncoated Ge. The ratio of these thresholds, 0.66 is still in consonance with the SW electric-field explanation. Although only two points are used in figure 7 to draw a straight line, the threshold dependence of both coated and uncoated Ge goes nearly as the square root of the Ge pulsewidth:

AR-coated Ge

$$\varepsilon_D = 0.455\ \tau^{0.52} \tag{5}$$

Uncoated Ge

$$\varepsilon_D = 0.67\ \tau^{0.53} \tag{6}$$

This scaling relationship is the same as that for free electron absorption in metallic surfaces for for electron plasma absorption initiated by avalanche breakdown in dielectrics [6].

7. Discussion

It is a general observation that the rear surface of transparent dielectric is damaged prior to the front surface, assuming the surfaces have identical surface properties and when the laser beam is not sharply focussed on either surface. For substrates like glass, this effect has been clearly demonstrated to be due to the greater standing-wave electric field at the rear surface [7]. Figure 8 illustrates the 180° phase reversal of the reflected wave at the front surface and the in-phase reflected wave at the back surface. The resultant ratio of the total electric fields at the two surfaces is

$$\frac{E(\text{rear})}{E(\text{front})} = \frac{2n}{n+1} , \tag{5}$$

a quantity greater than unity.

The magnitude of this field ratio for several dielectrics, transparent at 10.6 µm, is listed in table 6. As reported in section 1, only front surface damage of Ge was observed for all surfaces, AR-coated or uncoated, polycrystalline or single-crystal, doped or undoped. This was very surprising considering the large ratio, 1.60, for the fields. Even for a thinner (3 mm) substrate, no rear damage could be caused. To clarify this observation, three other substrates, NaCl, CdSe and CdTe, were irradiated. The expected early rear-surface damage was observed for NaCl and CdSe, but like Ge, only front surface damage could be produced on CdTe. This was especially intriguing since the band gap of CdTe and CdSe are nearly the same, ~ 1.6-1.7 eV [8].

Table 6. Rear versus front surface damage at 10.6 microns

Substrate	Refractive Index	Ratio of Electric Fields Rear to Front	Damage First Observed
NaCl	1.49	1.20	Rear
CdSe	2.43	1.42	Rear
CdTe	2.69	1.46	Front Only
Ge	4.0	1.60	Front Only

A first order examination of this phenomenan requires taking into account the gentle convergence of the laser beam at the sample and the linear absorption of the Ge using the relation for an uncoated substrate

$$\frac{E_2}{E_1} = \frac{2n_1}{n+1}\ \frac{w_1}{w_2}\ e^{-\alpha x/2}\ , \tag{6}$$

where 1,2 refer to front and rear surfaces, w is the spot size radius, α is the absorption coefficient and x is thickness. For our experiment $w_1/w_2 = 1.008$ and sample thicknesses were 5.6 mm. For the p-doped Ge, of resistivity 3 Ω. cm, the weak signal absorption was approximately 0.6 cm^{-1}.

Substituting, we find that E_2 was 1.15 times E_1 for weak intensities and larger for higher saturating intensities. For undoped, AR-coated Ge ($\alpha \simeq 0.005\ cm^{-1}$ at 10.6 μm), E_2 was 1.61 times E_1. Only in the case of AR-coated, p-doped Ge was E_2 less (between 0.72 and 1.0) than the E_1. However, attempts to damage the rear surface of these samples by increasing the incident laser intensity were unsuccessful.

One promising explanation for the absence of rear surface damage was suggested by Phipps [9]. In a darkened room he observed a faint blue surface corona on the front surface of a Brewster Ge plate well below the threshold for damage. This corona was distinctly different from a spark associated with an electron avalanche, and no traces of damage were found. It is possible that this visible light was emitted during carrier recombination. Further, absorption of this visible light by the Ge could increase the free carrier density for intrinsic Ge ($2 \times 10^{13}/cm^3$ at 300°K) to obtain a sufficiently absorbing plasma for higher laser intensities to cause surface damage. Further experiments are obviously needed to examine this possibility.

8. SUMMARY

This study has produced a number of results which are best listed under three headings.

5.1 GENERAL

a. The damage threshold was limited by germanium surface properties.

b. Front surface damage, only, occurred.

c. Pulsewidth dependence E_D (J/cm^2) $\sim\tau^{\frac{1}{2}}$ was observed between 1 and 70 ns.

5.2 BARE GE

a. The damage threshold at 1.2 ns ranged from 0.65 to 0.70 J/cm^2.

b. An HNO_3 treatment raised the threshold ~10%.

5.3 AR-COATED GE

a. Damage thresholds at 1.2 ns ranged from 0.41 to 0.57 J/cm^2, a span of 32%.

b. Multiple-shot conditioning (N-on-1) produced the same threshold as single shot tests (1-on-1).

c. No variation in threshold for 3 different conventional polished on substrates was observed.

d. No large difference of the threshold between substrates with varied doping or crystallinity was observed.

9. ACKNOWLEDGMENTS

The authors wish to thank the optics personnel of the optical companies listed in Table 6 for producing, polishing and AR-coating the Ge test substrates. Also, due credit are Ed Foley and Andrew Nowak for constructing and maintaining the CO_2 laser used in these tests and George Faulkner for technical assistance with the experiments. We add our appreciation to Claude Phipps for several helpful discussions.

Table 6. Participating Optical Companies

Germanium Substrates:

Eagle-Picher

Coatings:

Coherent radiation
Design Optics
Exotic Materials, Inc.
Honeywell, Inc.
Optical Coating Laboratory, Inc.
Perkin-Elmer Corporation
Santa Barbara Research
II-VI, Inc.
Valtec Corporation

Polishing:

Design Optics
Optical Systems & Technology, Inc.

10 References

[1] Phipps, C.R., Thomas, S.J. and Figuera, J.F., paper WAG, 1976 Conference on Laser and Electro optical Systems, Digest of Technical Papers, 30 (1976).

[2] Phipps, C.R., Thomas, S.J., Leyish, J., Czuchlewski, S.J., and Figuera, J.F., paper S.S, 1977 Conference on Laser Engineering and Applications, Digest of Technical Papers, 36 (1977).

[3] McLellan, E.J. and Lunsford, J.S., paper 8.10, ibid, 58 (1977).

[4] Jackson, J.D., Classical Electrodynamics, (John Wiley & Sons, New York, 1962), p. 295.

[5] Temple, P.A., and Soileau, M.J., NBS Spe. Pub. 462, 371 (1976).

[6] Bettis, J.R., House, R.A., and Guenther, A.H., NBS Spec. Pub. 462, 338 (1976).

[7] Crisp, M.D., NBS Spec. Pub. 387, 80 (1973).

[8] Pankove, J.I., Optical Processes in Semiconductors, (Prentice-Hall, Inc., Englewood Cliffs, NJ. 1971) pp. 412-413.

[9] Phipps, C.R., private communications, 1977.

[10] Wenzel, R.G., Arnold, G.P., and Greiner, N.R., Appl. Opt. 12, 2245 (1973).

[11] Glen Sherman, II-VI, Inc. private communications, 1977.

[12] Kildal, H. and Iseler, G.W., Appl. Opt. 15, 3062 (1976).

[13] Davit, J., NBS Spec. Pub. 387, 170 (1973).

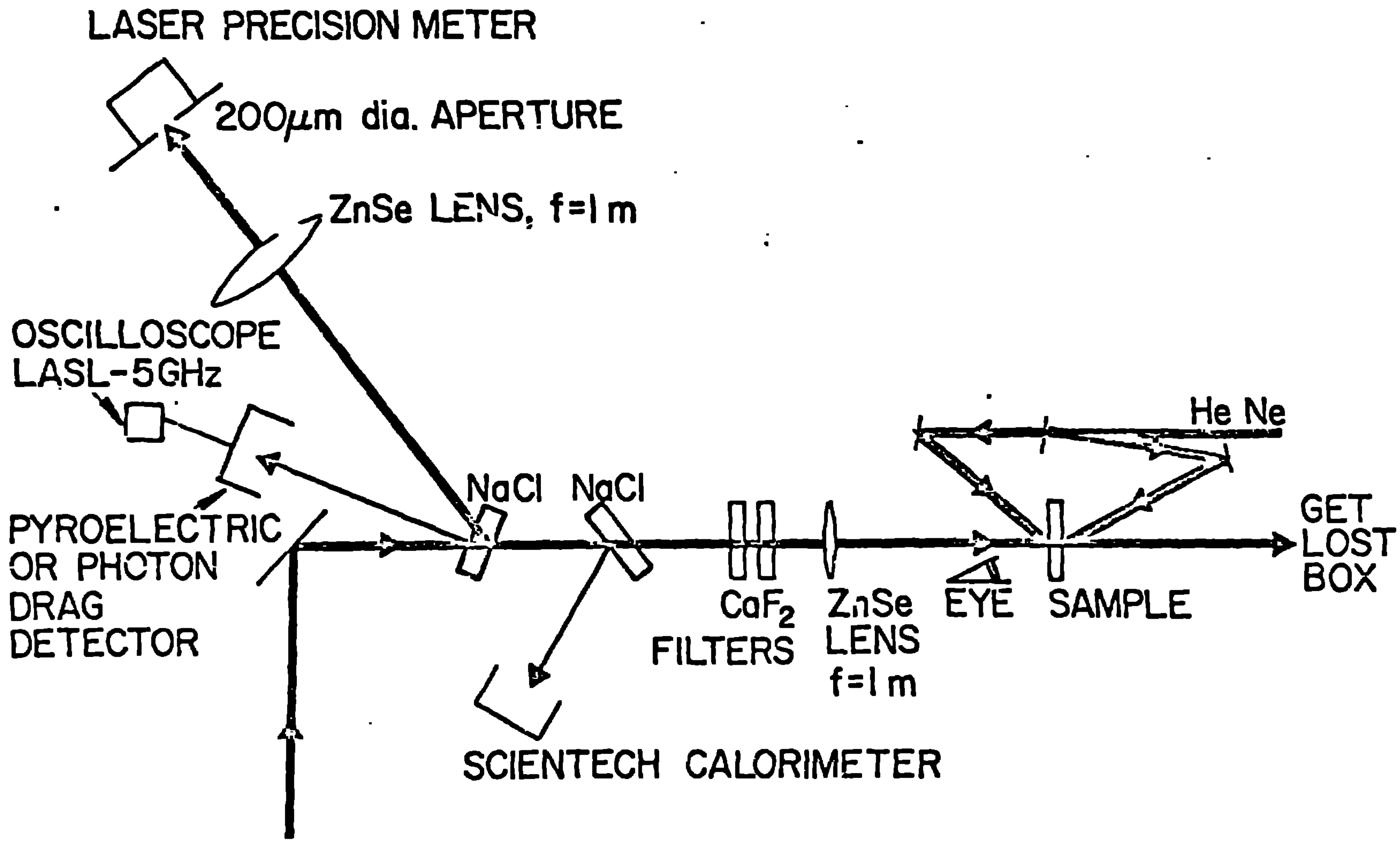

CO$_2$ LASER DAMAGE TEST FACILITY

Figure 1.

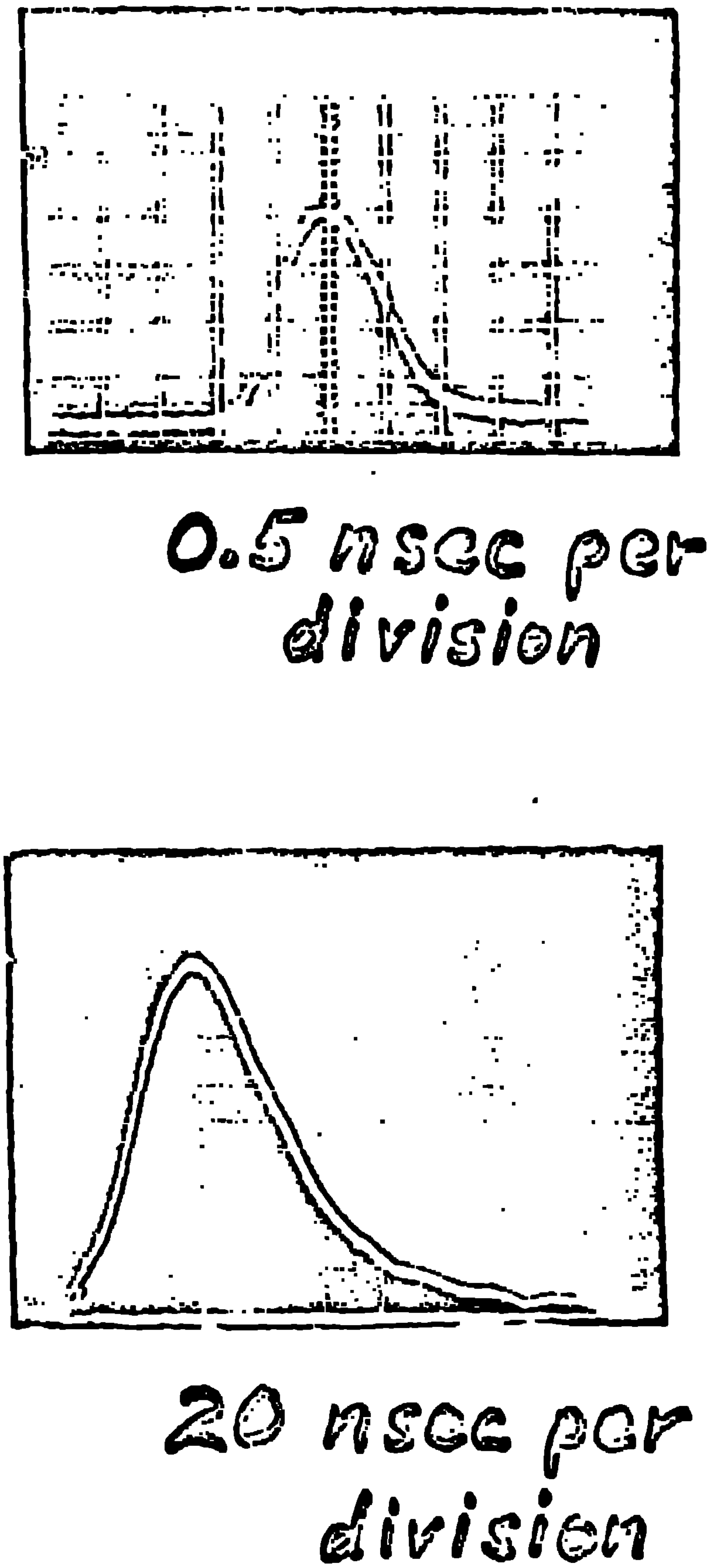

a.

b.

Figure 2.

Figure 3a.

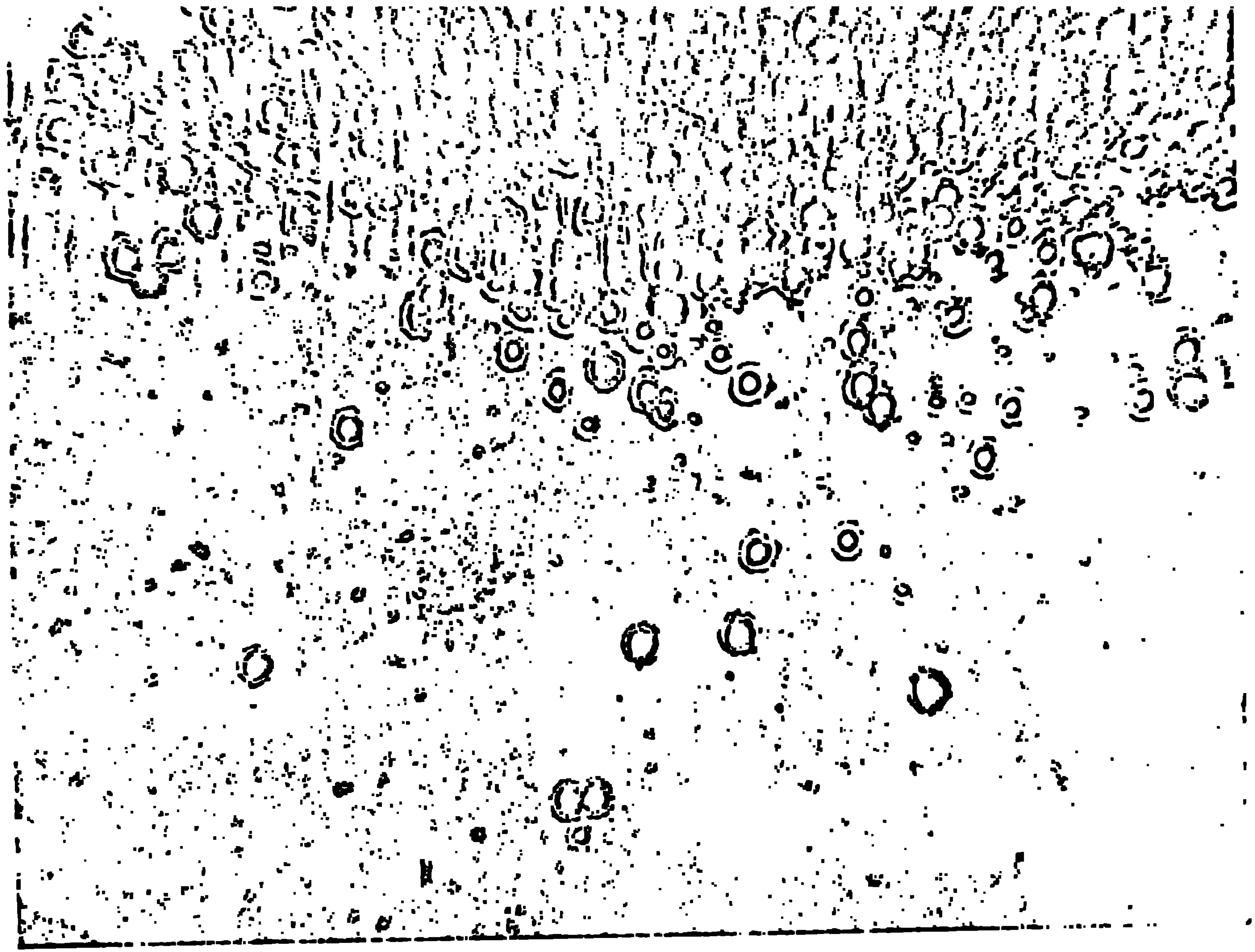

Figure 3b.

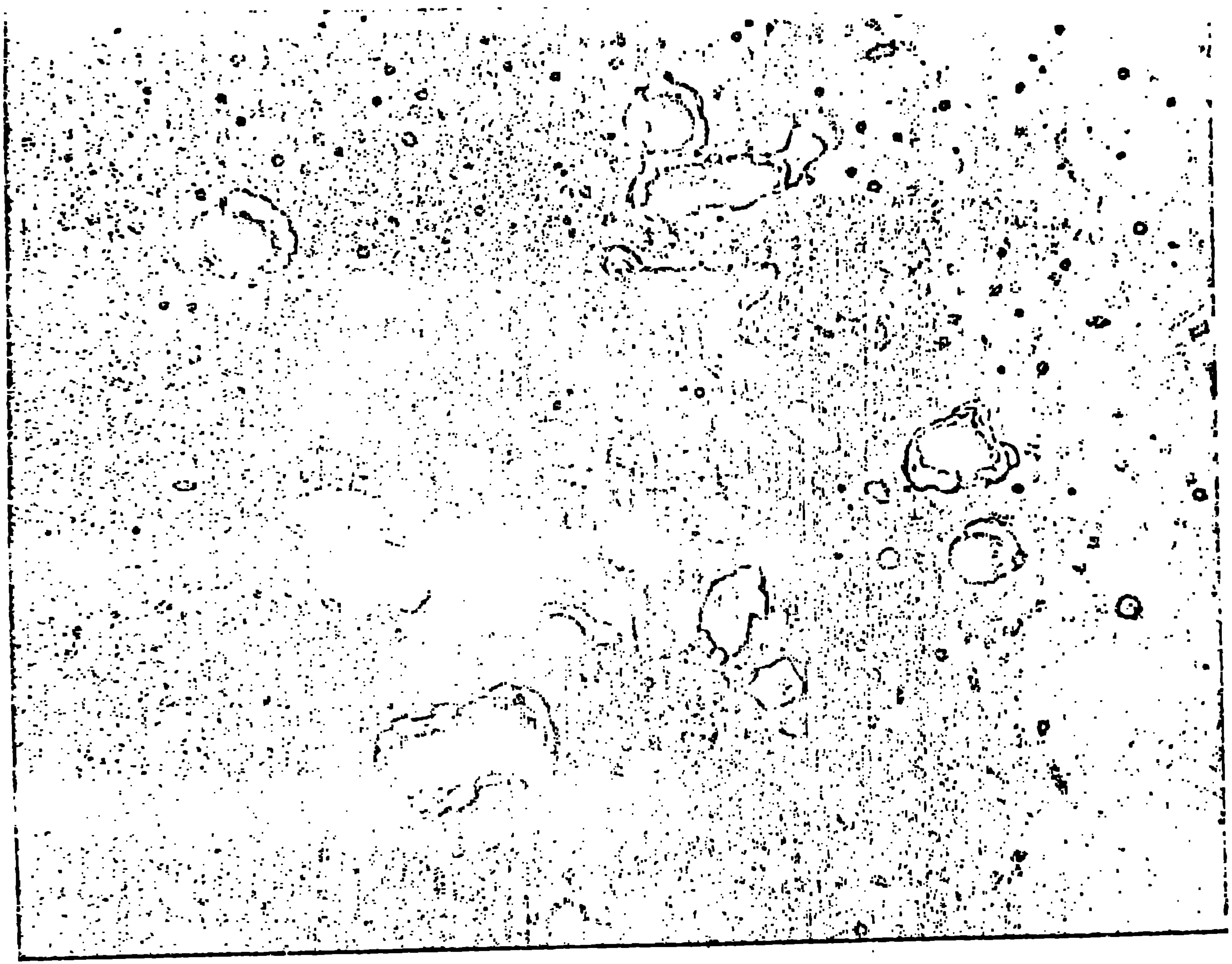

Figure 4a.

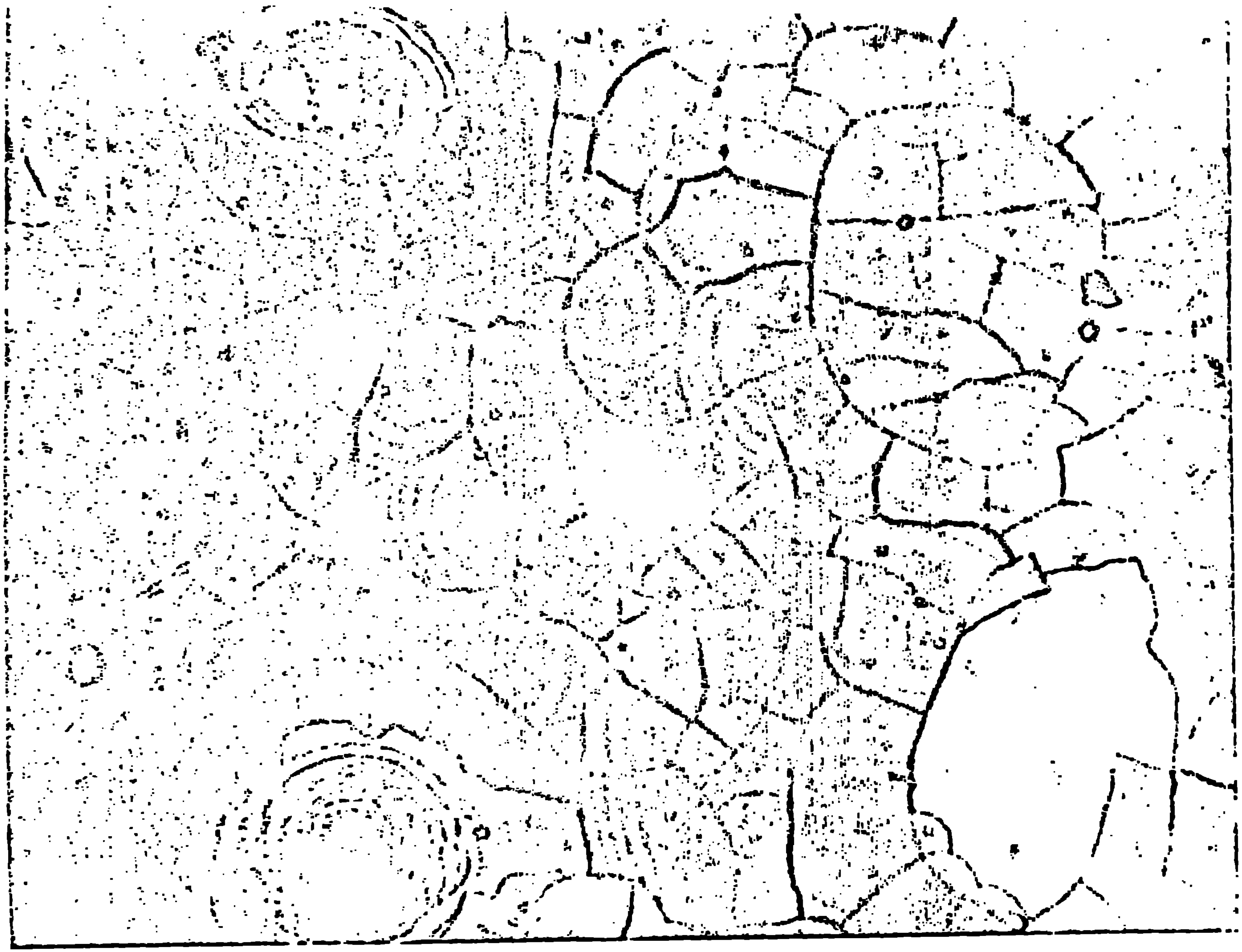

Figure 4b.

Figure 5a.

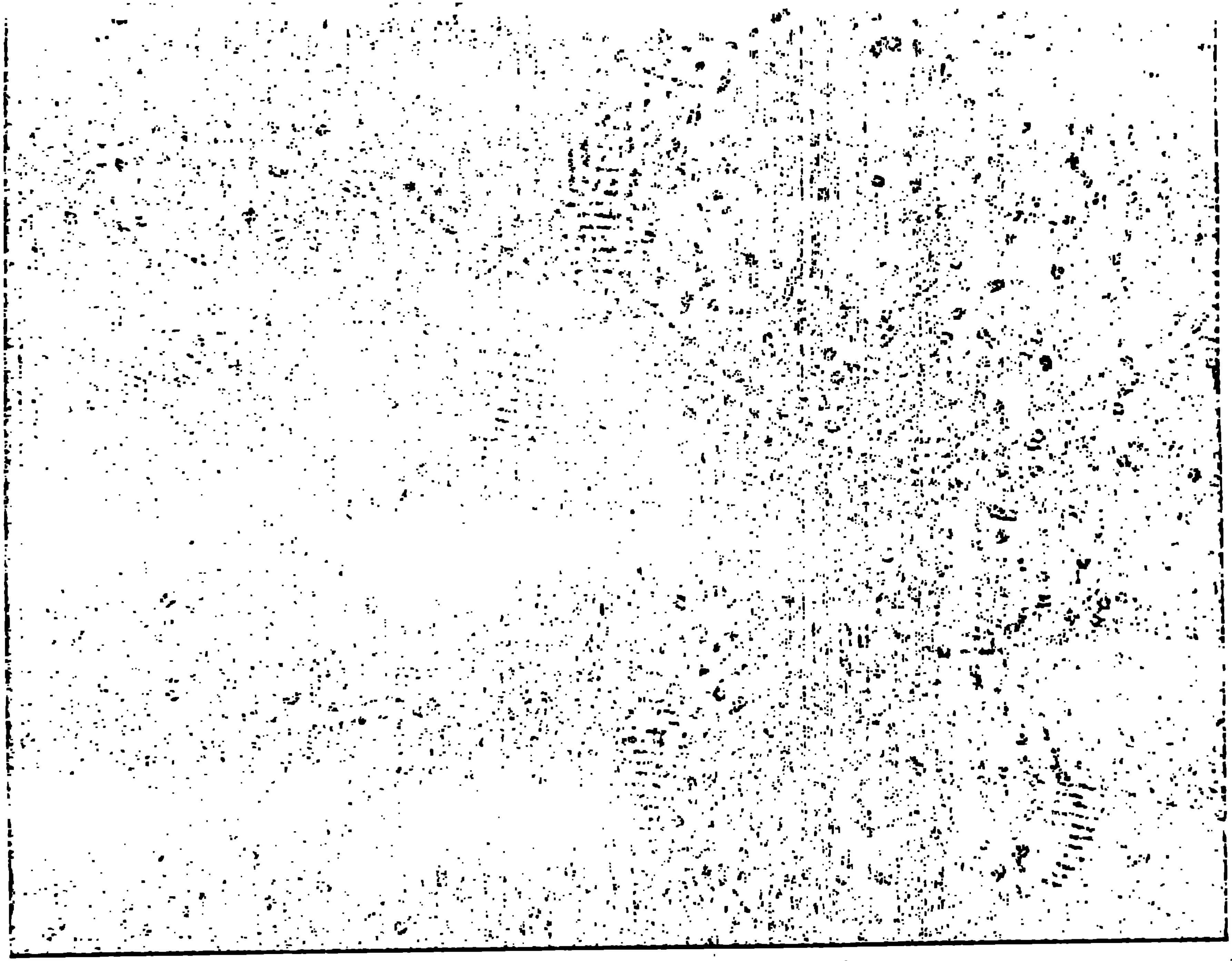

Figure 5b.

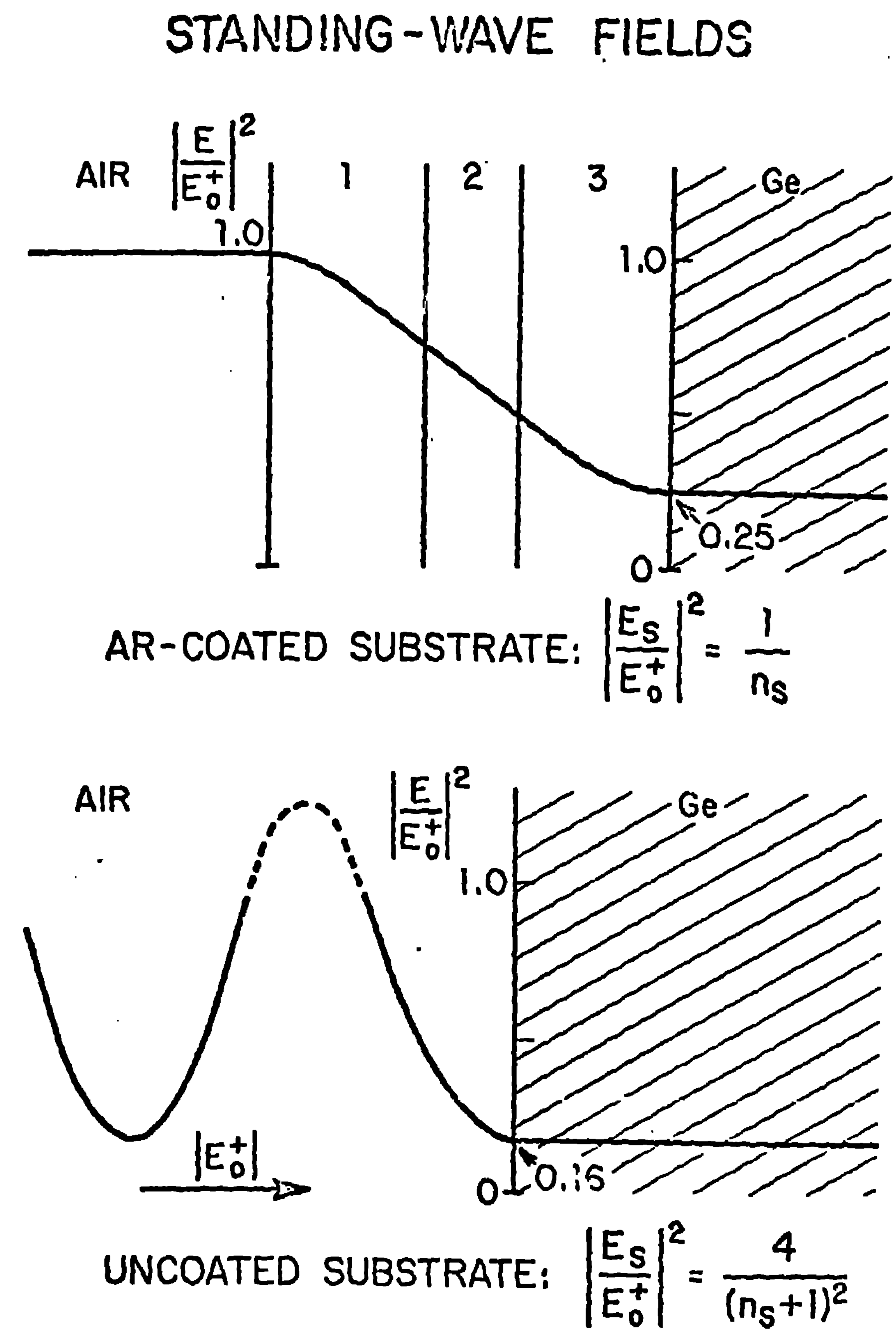
STANDING-WAVE FIELDS
AIR
$\left|\frac{E}{E_0^+}\right|^2$
1
2
3
Ge
1.0
1.0
0.25
0
AR-COATED SUBSTRATE: $\left|\frac{E_s}{E_0^+}\right|^2 = \frac{1}{n_s}$
AIR
$\left|\frac{E}{E_0^+}\right|^2$
Ge
1.0
$|E_0^+|$
0
0.16
UNCOATED SUBSTRATE: $\left|\frac{E_s}{E_0^+}\right|^2 = \frac{4}{(n_s+1)^2}$

Figure 6.

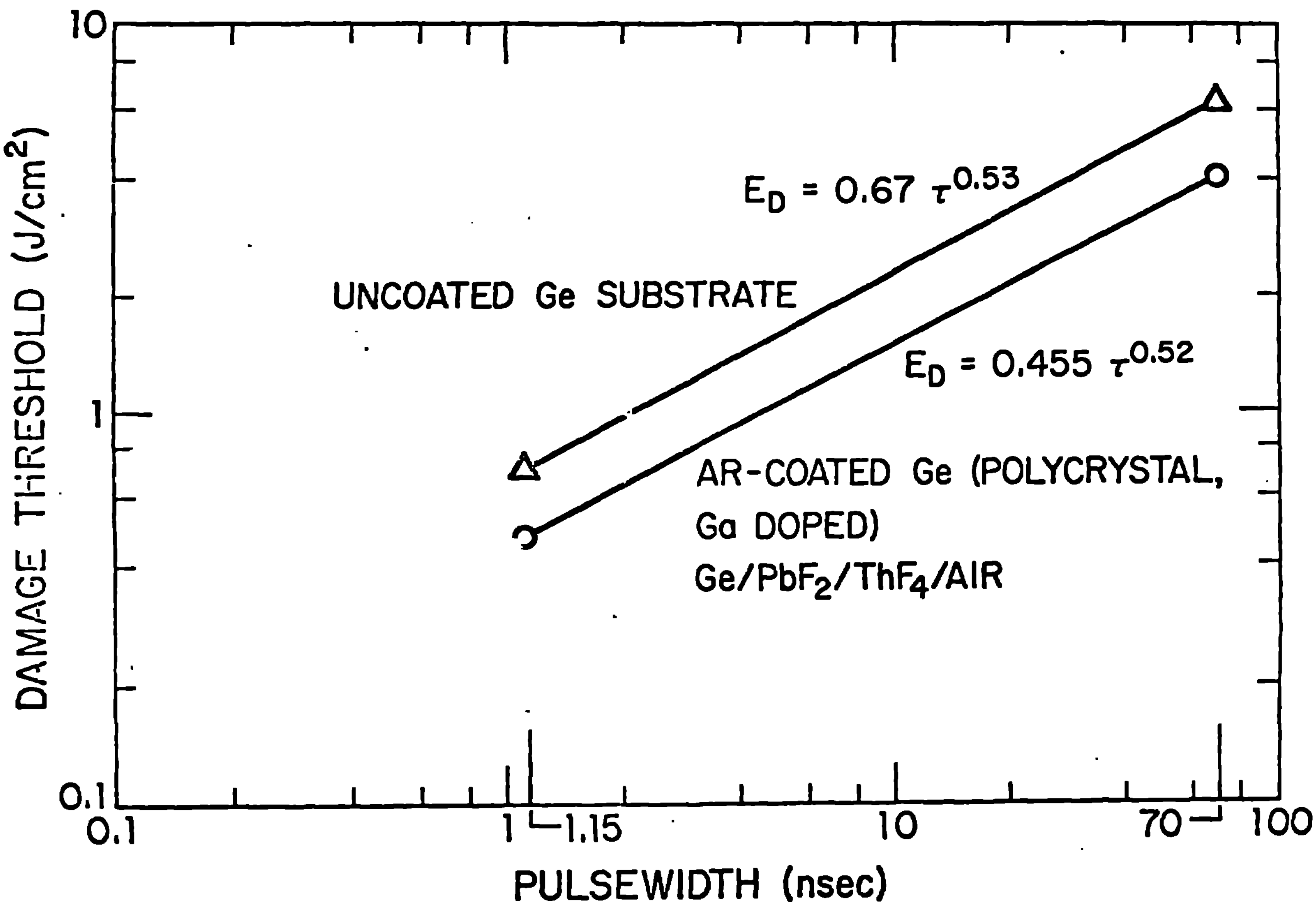
DAMAGE THRESHOLD (J/cm2)
PULSEWIDTH (nsec)
UNCOATED Ge SUBSTRATE
E_D = 0.67 τ^0.53
E_D = 0.455 τ^0.52
AR-COATED Ge (POLYCRYSTAL, Ga DOPED) Ge/PbF2/ThF4/AIR
0.1
1
10
0.1
1
1.15
10
70
100

Figure 7.

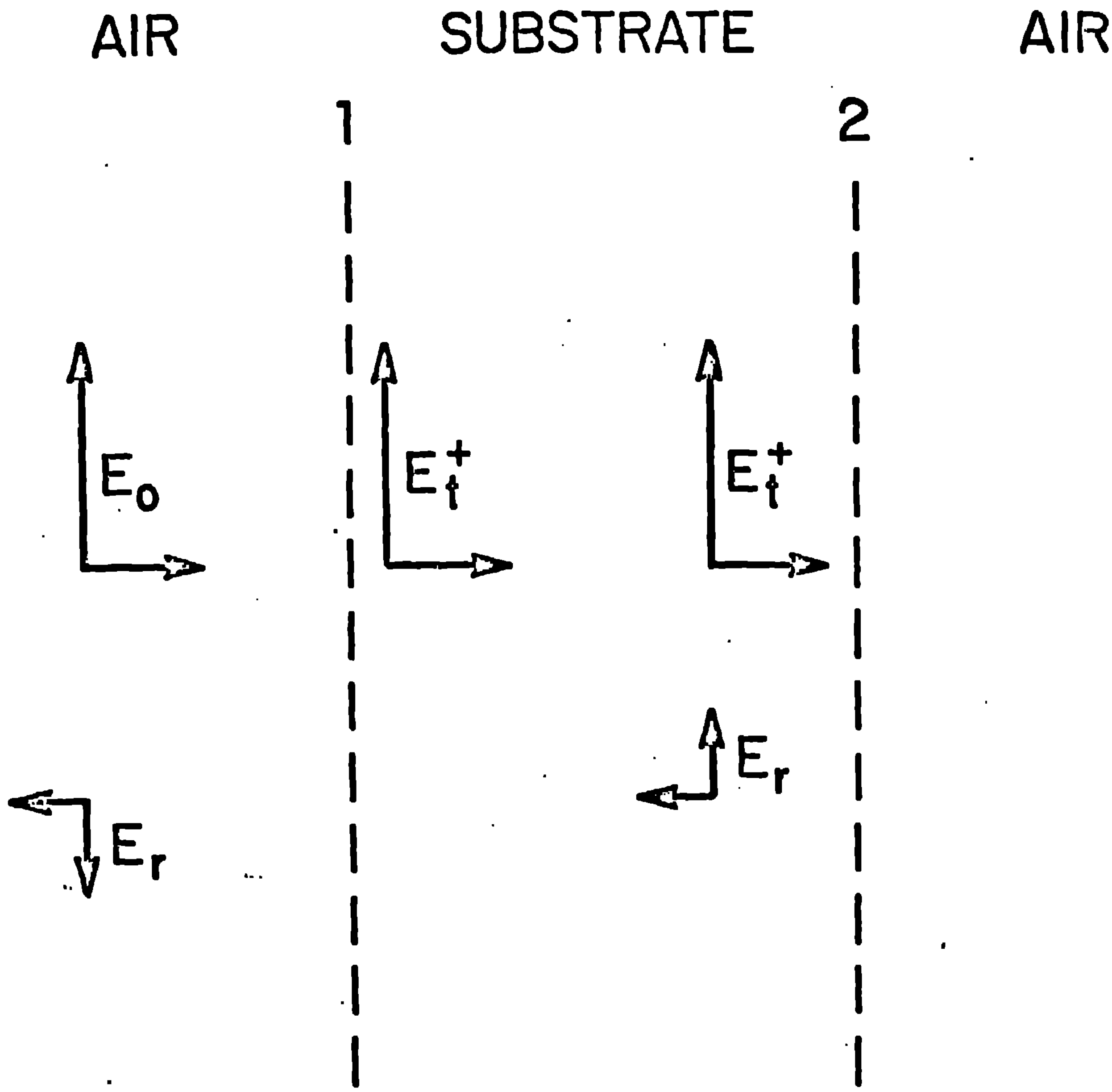

$$\frac{E\ (\text{REAR})}{E\ (\text{FRONT})} = \frac{2n}{n+1}$$

Figure 8.